Alpha-synuclein expression in GnRH neurons of young and old bovine hypothalami

Yvan Bienvenu Niyonzima[A], *Yuuki Asato*[A], *Tomoaki Murakami*[B], *and Hiroya Kadokawa*[A*]

[A] *Faculty of Veterinary Medicine, Yamaguchi University, Yamaguchi-shi, Yamaguchi-ken 1677-1, Japan*

Tel.: + 81 83 9335825; Fax: +81 83 9335938

[B] *Cooperative Department of Veterinary Medicine, Tokyo University of Agriculture and Technology, Tokyo, Japan.*

[*]*Correspondence to: Hiroya Kadokawa*

Faculty of Veterinary Medicine, Yamaguchi University, Yamaguchi-shi, Yamaguchi-ken 1677-1, Japan

Tel.: + 81 83 9335825; Fax: +81 83 9335938

E-mail address: hiroya@yamaguchi-u.ac.jp

Running head: Alpha synuclein and GnRH

ABSTRACT

Context: Understanding of central nervous system mechanisms related to age-related infertility remains limited. Fibril α-synuclein, distinct from its monomer form, is implicated in age-related diseases and propagates among neurons akin to prions.

Aims: We compared α-synuclein expression in gonadotropin-releasing hormone (GnRH)-expressing neurons (GnRH neurons) in the pre-optic area, arcuate nucleus, and median eminence of healthy heifers and aged cows to determine its role in age-related infertility.

Methods: We analysed mRNA and protein expression, along with fluorescent immunohistochemistry for GnRH and α-synuclein, followed by Congo red staining to detect amyloid deposits, and confocal microscopy.

Key results: Both mRNA and protein expressions of α-synuclein were confirmed by reverse transcription-polymerase chain reaction (RT-PCR) and western blots in bovine cortex, hippocampus, and anterior and posterior hypothalamus tissues. Significant differences in α-synuclein mRNA expression were observed in the cortex and hippocampus between young and old cows. Western blots showed five bands of α-synuclein, probably reflecting monomer, dimer, and oligomers, in the cortex, hippocampus, hypothalamus tissues, and there were significant differences in some bands between young and old cows. Bright-field and polarized light microscopy did not detect obvious amyloid deposition in aged hypothalami; however, higher-sensitive confocal microscopy unveiled strong positive signal of Congo red and α-synuclein in GnRH neurons in aged hypothalami. Additionally, α-synuclein expression was detected in immortalized GnRH neurons, GT1-7 cells.

Conclusion: α-synuclein was expressed in GnRH neurons, and some differences were observed between young and old hypothalami.

Implications: α-synuclein may play an important role in ageing-related infertility.

Keywords: Ageing, arcuate nucleus, Congo red staining, cortex, GT1-7 cell, hippocampus, median eminence, pre-optic area, ruminant.

Introduction

Ageing increases the chances of infertility in both humans (Gunes *et al*. 2016; van den Beld *et al*. 2018; Epelbaum and Terrien 2020) and cattle (Osoro and Wright 1992; Malhi *et al.* 2006). However, little is known of the central nervous system mechanisms pertaining to this phenomenon. Hypothalamic gonadotrophin-releasing hormone (GnRH) plays an essential role in reproductive function. The cell bodies of important GnRH neurons are located in the pre-optic area (POA), and fibres are projected to the arcuate nucleus (ARC) and median eminence (ME) to secrete GnRH peptide (Putteeraj *et al*. 2016). A great proportion of GnRH neurons (86%) are clustered with other GnRH neurons in the POA (Campbell *et al*. 2009). However, little is known regarding the changes that occur in these neurons with ageing.

α-synuclein is a protein encoded by the *SNCA* gene, which is synthesised as the brain advances from the foetal to mature stage (Raghavan *et al*. 2004; Sulzer and Edwards 2019; Jin *et al*. 2024). While the precise physiological functions and roles of native monomeric α-synuclein remain unclear (Jin *et al*. 2024), it has been observed to associate with synaptic vesicles (Sulzer and Edwards 2019) and interact with the ATP synthase subunit to enhance ATP synthase efficiency and mitochondrial function (Tripathi and Chattopadhyay 2019). The monomers of α-synuclein aggregate to form fibril α-synuclein, which causes brain disease with advancing age, including Alzheimer’s diseases, Parkinson's Disease, and Lewy body dementia (Fields *et al*. 2019; Ahmed *et al*. 2022; Deyell *et al.* 2023). Moreover, the interaction of α-synuclein oligomers with ATP synthase switches from physiological to pathological, resulting in mitochondrial dysfunction (Tripathi and Chattopadhyay 2019). Furthermore, aggregated α-synuclein damages cells (Fields *et al*. 2019) and lipid rafts in the plasma membrane

(Perissinotto *et al*. 2020). Importantly, α-synuclein propagates among neurons like prions (Melki 2018). However, no study to date has investigated whether α-synuclein propagates to the GnRH neurons and whether infected GnRH neurons synthesize α-synuclein.

Aged brains have amyloid depositions due to various causative molecules, including α-synuclein (Yanamandra *et al*. 2011; Marsh and Blurton-Jones 2012). The traditional method to visualise amyloid deposition is Congo red staining for bright-field and polarised light microscopy (green, yellow, orange, or red) (Obrenovich and Monnier 2004); however, recent studies have reported that the Congo red-positive region can be detected by higher-sensitivity confocal microscopy (Schultz *et al*. 2011; Scivetti *et al*. 2016; Castellani *et al*. 2017). Amyloid deposition was thought to occur only in the extracellular space, but a recent study on Lewy body dementia revealed that amyloid deposition can also occur in the cytoplasm of neurons (Araki *et al.* 2019). Congo red fluorescence is also detected inside neurons by fluorescence microscopy (Puladi *et al.* 2021). However, little is known about amyloid depositions in the hypothalamus. Interestingly, an intracerebroventricular injection of aggregated amyloid β fragment may damage ARC and ME in rats (Zussy *et al*. 2011), meaning that GnRH neurons may be affected by amyloid deposition.

To the best of our knowledge, no previous study has reported the expression of α-synuclein in GnRH neurons and how this expression differs between young and old hypothalami. Therefore, we compared α-synuclein expression in the GnRH neurons of POA, ARC, and ME between healthy heifers and old cows to estimate the importance of α-synuclein for infertility with ageing. Additionally, we confirmed α-synuclein expression in the well-known immortalized GnRH neuron model, GT1-7 cells (Liposits

100 *et al*. 1991).

101

102 **Materials and Methods**

103 *Animals and treatments*

104 All experiments were performed according to the Guiding Principles for the Care
105 and Use of Experimental Animals in the Field of Physiological Sciences (Physiological
106 Society of Japan) and approved by the Committee on Animal Experiments of
107 Yamaguchi University (approval number 301).

108 All cattle were managed by our contracted farmer in western Japan. The farm had
109 open free-stall barns with free access to water. The cattle were fed twice daily with a
110 total mixed ration according to the Japanese feeding standard (Agriculture, Forestry and
111 Fisheries Research Council Secretariat, 2022). Following the disaster of bovine
112 spongiform encephalopathy in 2002, all cattle born in Japan are registered at birth in a
113 national database, each with a unique identification number. Consumers can obtain
114 information about the breed, date of birth, farm of origin, and slaughter by querying the
115 server of the National Livestock Breeding Centre of Japan. We verified this information
116 for all cattle involved in this study. All cattle were slaughtered at a local abattoir to
117 harvest beef according to the regulation of the Ministry of Agriculture, Forestry, and
118 Fisheries of Japan. All cattle were non-lactating, non-pregnant, and with no follicular
119 cysts, luteal cysts, or other ovarian disorders, based on macroscopic examination of the
120 ovaries (Kamomae 2012). Among 2,600 Japanese Black heifers, the average pregnancy
121 period was 9 months, while the minimum age at first calving was 21.4 months (Inoue *et*
122 *al.* 2020); thus, the cattle are sexually mature after about 15 months.

123 We obtained brain samples [cortex, hippocampus, anterior hypothalamus (AH) block

containing the POA, and posterior hypothalamus (PH) block containing the ARC and ME] from healthy post-pubertal Japanese Black heifers (22.6 ± 1.5 months of age; *n*=5; young group) and old Japanese Black cows (164.8 ± 5.0 months of age; *n*=5; old group) using methods detailed in our previous studies (Kadokawa *et al*. 2014; Kereilwe and Kadokawa 2020a, 2020b; Niyonzima *et al.* 2024). The above-mentioned samples (from four Japanese Black heifers and four old Japanese Black cows) were also used in another study conducted by our group (Niyonzima *et al.* 2024). The AH and PH blocks used in the present study are equivalent to the blocks labelled as "anterior hypothalamus containing the suprachiasmatic nucleus (SCN) and supraoptic nucleus (SON), and posterior hypothalamus containing the paraventricular hypothalamic nucleus (PVN) and SON," respectively, in the above-mentioned paper. We collected samples of the cortex from the frontal lobe, caudal to the central sulcus near the midline. The hippocampus samples were collected from the temporal lobe, ventral to the lateral ventricle, after identifying it by its unique shape (Rech *et al*. 2018). We used samples obtained in the middle luteal phase, i.e., 8 to 12 days after ovulation, as determined by macroscopic examination of the ovaries and uterus (Miyamoto *et al*. 2000). It should be noted that there is no difference in GnRH immunoreactivity in the bovine POA, ARC, and ME between the periestrus and diestrus phases (Tanco *et al*. 2016). Old cows were slaughtered after completing parturition enough times as planned by farmers to obtain beef, usually after 10 years of age. Each block was stored in 4% paraformaldehyde at 4°C for 24 h. The fixed blocks were placed in a 20% sucrose solution at 4°C for 72 h. They were then stored in 30% sucrose solution at 4°C until the block sank – at least 48 h.

We also collected cortex, hippocampus, AH and PH tissue samples from other healthy

148 post-pubertal Japanese Black heifers (22.5 ± 1.3 months of age; *n*=6; young group) and
149 old Japanese Black cows (160.7 ± 10.8 months of age; *n*=6; old group) to perform reverse
150 transcription-polymerase chain reaction (RT-PCR), quantitative RT-PCR, and western
151 blot analyses. The above-mentioned samples were also used in another study (Niyonzima
152 *et al.* 2024). Both AH and PH blocks were cut at the midline to obtain left and right sides.
153 Using the bovine brain atlas (Leshin *et al.* 1988; Okamura 2002) as a reference, the blocks
154 were further cut using their exterior shapes and the third or lateral ventricles as landmarks.
155 Finally, the size of each AH tissue sample was less than 1 cm along the lateral axis; 2 cm
156 along the rostrocaudal axis; and 3 cm along the vertical axis. The size of each PH tissue
157 sample was less than 1 cm along the lateral axis; 2 cm along the-rostrocaudal axis; and 1
158 cm along the vertical axis. The AH and PH tissues were immediately frozen in liquid
159 nitrogen and stored at −80°C until RNA or protein extraction.
160
161 *Cell Culture for GT1-7cells*
162 The mouse neuronal cell line, GT1-7 was a generous gift from Dr. Pamela Mellon
163 (Liposits *et al*. 1991). The cells were maintained in Dulbecco's Modified Eagle's Medium
164 (DMEM; 12430054, Thermo Fisher Scientific, Waltham, MA, USA), supplemented with
165 10% foetal bovine serum, 100 U/mL penicillin, and 50 μg/mL streptomycin. All cells
166 were grown in a humidified incubator at 37°C with 5% CO_2. GT1-7 cells were used for
167 RT-PCR to evaluate α-synuclein mRNA expression.
168
169 *RT-PCR, sequencing of amplified products, and homology search in gene databases*
170 We used a previously reported method of RT-PCR used in bovine brains
171 (Niyonzima *et al*. 2024). Briefly, total RNA was extracted from the samples of cortex,

hippocampus, AH, and PH tissues (n = 6 per group per region), or GT1-7 cells using RNAzol RT isolation reagent (Molecular Research Centre Inc., Cincinnati, OH, USA) according to the manufacturer's protocol. The extracted RNA samples were treated with ribonuclease-free deoxyribonuclease (Toyobo, Tokyo, Japan) to eliminate possible genomic DNA contamination. Using a NanoDrop ND-1000 spectrophotometer (NanoDrop Technologies Inc., Wilmington, DE, USA), the concentration and purity of each RNA sample were evaluated to ensure the A_{260}/A_{280} nm ratio was in the acceptable range of 1.8–2.1. The mRNA quality of all samples was verified by electrophoresis of total RNA followed by staining with ethidium bromide, and the 28S:18S ratios were 2:1. The complementary deoxyribonucleic acid (cDNA) was synthesized using the Verso cDNA Synthesis Kit (Thermo Fisher Scientific).

To determine the expression of *SNCA* mRNA in bovine brain samples or GT1-7 cells, PCR was conducted using primers designed by the Primer3 algorithm based on the reference sequences of bovine *SNCA* (National Centre for Biotechnology Information [NCBI] reference sequence of bovine *SNCA* is NM_001034041.2) or mouse *SNCA* (NM_001042451.2). Table 1 shows the details of the primers, which were also used in a previous study on bovine brains (Niyonzima *et al.* 2024). The expected PCR-product sizes of bovine and mouse *SNCA* using the primer pairs are 303 bp and 306 bp, respectively. Using a Veriti 96–Well Thermal Cycler (Thermoscientific), PCR was performed using 50 ng of cDNA and polymerase (Tks Gflex DNA Polymerase, Takara Bio Inc., Shiga, Japan) under the following thermocycles: 94°C for 1 min for pre-denaturing followed by 35 cycles of 98°C for 10 s, 60°C for 15 s, and 68°C for 30 s. PCR products were separated on 1.5% agarose gel by electrophoresis with a molecular marker [Gene Ladder 100 (0.1–2 kbp), Nippon Gene, Tokyo, Japan], stained with fluorescent

196 stain (Gelstar, Lonza, Allendale, NJ, USA), and observed using a charge-coupled device
197 (CCD) imaging system (GelDoc; Bio-Rad, Hercules, CA, USA). The PCR products were
198 purified with the NucleoSpin Extract II kit (Takara Bio Inc.) and then sequenced with a
199 sequencer (ABI3130, Thermo Fisher Scientific) using one of the PCR primers and Dye
200 Terminator v3.1 Cycle Sequencing Kit (Thermo Fisher Scientific). The sequences
201 obtained were used as query terms with which to search the homology sequence in the
202 NCBI database using the basic nucleotide local alignment search tool (BLAST) optimized
203 for highly similar sequences.
204
205 *Quantitative RT-PCR for SNCA*
206 We used a previously reported method of quantitative RT-PCR for bovine brains
207 (Niyonzima *et al.* 2024). Briefly, after preparation of high-quality total RNA and cDNA
208 synthesis using the previously described protocol, *SNCA* mRNA expression levels in the
209 cortex, hippocampus, AH, and PH tissues were compared between the young and old
210 groups via quantitative RT-PCR and data analyses as described previously (Kadokawa *et*
211 *al.* 2021). The expression of each enzyme was normalised against the geometric mean of
212 the expression of two housekeeping genes, *tyrosine 3-monooxygenase/tryptophan 5-*
213 *monooxygenase activation protein zeta* (*YWHAZ*; NCBI reference sequence,
214 NM_174814.2) and *succinate dehydrogenase complex flavoprotein subunit A* (*SDHA*;
215 NCBI reference sequence, NM_174178.2). These two housekeeping genes were selected
216 as the most stable and reliable housekeeping genes to use in the bovine hypothalamus
217 (Kadokawa *et al*. 2021), and cortex and hippocampus of sheep and rats (Bonefeld *et al*.
218 2008; Gossner *et al.* 2011).
219 The amount of gene expression was measured in duplicate by quantitative RT-

PCR analyses with 50 ng cDNA, using CFX96 Quantitative RT-PCR System (Bio-Rad) and Power SYBR Green PCR Master Mix (Thermo Fisher Scientific), together with a 6-point relative standard curve, non-template control, and no reverse-transcription control. Standard 10-fold dilutions of purified and amplified DNA fragments were prepared. Temperature conditions for all genes were as follows: 95°C for 10 min for pre-denaturation; five cycles each of 95°C for 15 s and 66°C for 30 s; and 40 cycles each of 95°C for 15 s and 60°C for 60 s. Melting curve analyses were performed at 95°C for each amplicon and each annealing temperature to ensure the absence of smaller non-specific products such as dimers. To optimize the quantitative RT-PCR assay, serial dilutions of a cDNA template were used to generate a standard curve by plotting the log of the starting quantity of the dilution factor against the Cq value obtained during amplification of each dilution. All the Cq values of the unknown samples (23.9 ± 0.2) were between the highest (8.0) and lowest (31.0) standards for *SNCA* in quantitative RT-PCR. Further, all the Cq values of the unknown samples were between the highest and lowest standards for *YWHAZ* and *SDHA* in quantitative RT-PCR. Reactions with a coefficient of determination (R2) > 0.98 and efficiency between 95 and 105% were considered optimized. The coefficients of variation of quantitative RT-PCRs were less than 6%. The concentration of PCR products was calculated by comparing the Cq values of unknown samples with the standard curve using appropriate software (CFXmanagerV3.1, Bio-Rad). Then, the *SNCA* amount was divided by the geometric mean of *YWHAZ* and *SDHA* in each sample.

Antibodies

The human/rat/mouse α-synuclein rabbit polyclonal antibody (GTX112799; GeneTex, Inc., Irvine, CA, USA) recognizes human α-synuclein (NP_001029213.1). This antigen

sequence had 95% homology with bovine α-synuclein (NP_001029213.1) but no homology with other bovine proteins, as determined using protein BLAST. This antibody was used previously for western blots and immunohistochemistry in bovine brains (Niyonzima *et al.* 2024).

We also used an anti-GnRH mouse monoclonal antibody (clone number GnRH I HU11B: sc-32292, Santa Cruz Biotechnology, Inc., Dallas, TX, USA) raised against a synthetic GnRH I decapeptide by Urbanski (1991). This antibody was used for immunohistochemistry to visualize GnRH neurons in the bovine brain (Kereilwe and Kadokawa 2020a).

Western blotting for α-synuclein detection

We used a previously reported method of western blotting for the bovine brain (Kereilwe and Kadokawa 2020a, 2020b; Niyonzima *et al.* 2024). Briefly, proteins were extracted from the frozen-stock cortex, hippocampus, AH, and PH of young and old bovine groups (n=6 per region per group) utilizing a mortar, liquid nitrogen, and tissue protein extraction reagent (T-PER; Thermo Fisher Scientific) with protease inhibitors (Halt Protease Inhibitor Cocktail; Thermo Fisher Scientific). Proteins were also extracted from the whole brain of female mouse (5 weeks of age, B6C3F1/Slc, Japan SLC, Inc., Shizuoka, Japan) and used as a positive control. The total protein content of each tissue homogenate was estimated using the bicinchoninic acid kit (Thermo Fisher Scientific). The extracted protein samples were boiled with a sample buffer solution with reducing reagent (6x) for SDS-PAGE (09499-14; Nacalai Tesque, Kyoto, Japan) for 3 min at 100°C. Protein samples (8,000 ng of total protein) were loaded onto a sodium dodecyl sulphate–polyacrylamide gel (4–15% Criterion TGX gel, Bio-Rad) alongside a molecular weight

marker (Multicolour Protein Ladder; Nippon Gene Co. Ltd., Tokyo, Japan). Gels were run at 100 V for 90 min. Proteins were transferred onto polyvinylidene fluoride (PVDF) membranes via electroblotting at 1.0 A, 25 V, for 30 min using the Trans-Blot Turbo system (Bio-Rad). The PVDF membrane was stained with Revert 700 total protein stain (LI-COR Biosciences, Lincoln, NE, USA) for 5 min. After two 30-s washing cycles with 30% methanol containing 6.7% acetic acid, the PVDF membrane was neutralized with 10 mM Tris–HCl (pH 7.6) and 150 mM NaCl. Subsequently, the membrane was scanned using Odyssey CLx (LI-COR Biosciences) to calculate the total protein content using Image Studio ver3 software (LI-COR Biosciences).

The Can Get Signal Immunoreaction Enhancer kit (Toyobo Co. Ltd, Osaka, Japan) served as a blocking agent (1 h at 25°C) for the primary antibody reaction (16 h at 4°C) with the anti-α-synuclein antibody (1:100,000 dilution in 20 ml of immunoreaction enhancer solution I supplemented with 20 μg normal goat IgG [Wako Pure Chemicals, Osaka, Japan]) and secondary antibody reaction (1 h at 25 °C) with the goat anti-rabbit IgG horseradish peroxidase-conjugated antibody (Bethyl Laboratories Inc., Montgomery, TX, USA; 1:100,000 dilution in 20 ml of immunoreaction enhancer solution II supplemented with 20 μg normal goat IgG).

Protein bands were visualized using the Amersham ECL-Prime chemiluminescence kit (Cytiva, Marlborough, MA, USA) and CCD imaging system (Amersham Image Quant 800, Cytiva). To verify signal specificity, several negative controls were included, wherein the primary antibodies were omitted, or normal rabbit IgG was used instead of the primary antibodies. Signal specificity was also confirmed using negative controls in which the primary antibodies were pre-absorbed with 5 nM of the antigen peptide (Scrum Inc., Tokyo, Japan). ImageQuant TL (version 8.2; Cytiva)

292 software was used to measure the band sizes and volumes (calculated using rolling ball
293 background subtraction). The protein amount of α-synuclein was normalized against the
294 total protein.
295
296 *Cryosection*
297 After sucrose treatment, serial coronal sections were cut into 10 μm (for Congo red
298 staining) or 50 μm thick (for immunohistochemistry followed by Congo red staining)
299 sections using a cryostat (CM1900, Leica Microsystems Pty Ltd., Wetzlar, Germany)
300 based on a previously reported method (Kereilwe and Kadokawa 2020a) and using an
301 atlas of bovine brain sections as a guide (Leshin *et al.* 1988; Okamura 2002). Sections
302 were monitored in both the anterior and lateral views to identify the shape of the third
303 ventricle and the ventral or dorsal edge line, and to locate the anterior commissure, optic
304 chiasm, mammillothalamic tract, and fornix. The selected AH tissues contained both the
305 anterior commissure and optic chiasm, and were medial or lateral to the third ventricle.
306 The selected PH tissues contained the fornix and were adjacent to both the evident
307 infundibular recess of the third ventricle and the median eminence, which is attached to
308 the infundibulum. Every sixth section of the tissue was subjected to staining for α-
309 synuclein, GnRH, and Congo red. At least four sections–from the rostral end of the
310 organum vasculosum of the lamina terminalis to the rostral edge of the hypothalamic
311 paraventricular nucleus were used for the AH block. At least four sections from the rostral
312 edge of the dorsomedial hypothalamic nucleus to the rostral edge of the mammillary
313 bodies were used for the PH block. The 50 μm thick sections were then stored in 25 mM
314 PBS containing 50% glycerol, 250 mM sucrose, and 3.2 mM $MgCl_2 \cdot 6H_2O$ at -20°C for
315 immunohistochemistry. The 10 μm thick sections were affixed to slide glass (MAS coat

316 Superfrost, Matsunami-Glass, Osaka, Japan).

317

318 *Congo red staining*

319 We used a previously reported method of Congo red staining used for bovine brains
320 (Niyonzima *et al*. 2024). Briefly, the slides with the 10 μm thick sections were covered
321 with haematoxylin (New Type M, Muto Pure Chemicals Co. LTD., Tokyo, Japan) for 2
322 min. After washing with water, Congo red solution (New Type M, Muto Pure Chemicals
323 Co. LTD.) was applied for staining for 3 min. The sections were rinsed twice with water
324 and differentiated by 0.2% potassium hydroxide in 80% ethanol (alkaline ethanol) for 3
325 seconds; then, the sections were dehydrated with 70%, 90%, 100%, and 100% ethanol,
326 and cleared with three changes of xylene. Excessive treatment with alkaline ethanol can
327 damage the brain structure, especially the ME. After attaching the coverslip with Entellan
328 new mounting medium (Sigma-Aldrich, St. Louis, MO, USA), the stained sections were
329 observed under both bright field and polarized light using a microscope (Eclipse Si, Nikon,
330 Tokyo, Japan) with a digital camera (MC120 HD, Leica Microsystems).

331

332 *Fluorescent immunohistochemistry and confocal microscopy*

333 The frozen-stock brain tissue was thawed and washed twice with PBS. Free-floating
334 tissue sections were permeabilized with PBS containing 0.5% Tween 20 for 3 min. Two
335 quenching methods were combined, glycine/hydrogen peroxide (Kereilwe and Kadokawa
336 2020a, 2020b) and Vector True VIEW autofluorescence quenching kit (Vector
337 Laboratories Inc., Burlingame, CA, USA), because tissue autofluorescence was observed
338 in a preliminary study. The tissue was blocked with PBS containing 2% normal goat
339 serum, 50 mM glycine, 0.05% Tween 20, 0.1% Triton X-100, and 0.1% BSA for 30 min

(Kereilwe and Kadokawa 2020a). The sections were then incubated with a cocktail of primary antibodies (anti-GnRH mouse and anti-α-synuclein rabbit antibodies [all diluted 1:1,000]) dissolved in PBS containing 10 mM glycine, 0.05% Tween 20, 0.1% Triton X-100, and 0.1% hydrogen peroxide at 4°C for 16 h. After the primary antibody incubation, the sections were washed once with PBS containing 0.5% Tween 20 (PBST) and twice with PBS, then incubated with a cocktail of fluorochrome-conjugated secondary antibodies (Alexa Fluor 488 goat anti-rabbit IgG, and Alexa Fluor 647 goat anti-mouse IgG [all from Thermo Fisher Scientific and diluted to 1 μg/mL]) and 1 μg/mL of 4′, 6′-diamino-2-phenylindole (DAPI; Wako Pure Chemicals) for 4 h at room temperature. After the secondary antibody incubation, the sections were washed once with PBST, and twice with PBS, and then each free-floating section was transferred onto a slide glass. For POA and A & M, the section was transferred onto a slide glass with the dorsal-ventral axis of the bovine brain section parallel to the long axis of the slide. After drying overnight, the section was stained with Congo red solution (New Type M, Muto Pure Chemicals Co. LTD.) for 3 min. The sections were rinsed twice with water, differentiated by alkaline ethanol for 3 seconds, washed with water, and stained with PBS containing 1 μg/mL of DAPI again for 10 min. The second DAPI staining was required because the first DAPI staining resulted in a weak DNA signal. Vector True VIEW autofluorescence quenching kit was subsequently employed, following the manufacturer's protocol. After 5 min of incubation with the quenching kit, the sections were rinsed twice with PBS. A cover glass (55 × 24 mm, Matsunami-Glass) was then attached using ProLong Glass Antifade Mountant (Thermo Fisher Scientific).

The sections were observed under a confocal microscope (LSM710; Carl Zeiss, Göttingen, Germany) equipped with a 405 nm diode laser, 488 nm argon laser, 533 nm

364 HeNe laser, and 633 nm HeNe laser. Images obtained by fluorescence microscopy were
365 scanned with a 20× or 40× oil-immersion objective and recorded with a CCD camera
366 system controlled by ZEN2012 Black Edition software (Carl Zeiss). Congo red staining
367 was viewed at 546 nm with the helium-neon laser (Schultz *et al.* 2011; Scivetti *et al*. 2016;
368 Castellani *et al.* 2017). GnRH, α-synuclein, and Congo red localization were examined in
369 confocal images of triple-labelled specimens. To verify the specificity of the signals, we
370 included several negative controls in which the primary antiserum had been omitted or
371 pre-absorbed with 5 nM of the antigen peptide, or in which normal rabbit IgG (Wako Pure
372 Chemicals) was used instead of the primary antibody.

373 We defined various segments of neurons based on the following criteria: the cell body
374 is round or polygonal in shape and has a diameter of more than 8 μm; fibre is shown as a
375 continuous line or dotted line of immunopositive signal. We identified a GnRH neuron if
376 the neuron had a shape similar to that reported in a previous paper on bovine GnRH
377 neurons (Kereilwe and Kadokawa 2020a) and showed a GnRH-positive signal.

378 We utilized the intensity measurement feature in the histogram functions of ZEN2012
379 Black Edition software. We defined the intensity as 'strong' if the arithmetic mean of the
380 fluorescent signal intensity in any region of interest (ROI) was at least 100 times higher
381 than the background, and 'weak' if it was less than 10 times higher than the background
382 signal.

383 To evaluate colocalization, the GnRH signal was shown in red and either α-synuclein
384 or Congo red was shown in green. Therefore, yellow coloration in the images indicated
385 colocalization of GnRH with α-synuclein or Congo red. The percentage of cell bodies or
386 fibres of GnRH single-labelled neurons and the percentage of double/triple-labelled cell
387 bodies or fibres of neurons among all of the GnRH-positive cell bodies or fibres of

neurons were determined in the POA, ARC, or ME of each heifer and cow. From each individual, four sections containing the POA and four sections containing the ARC and ME with a similar shape to those shown in the bovine brain atlas (Leshin *et al*. 1988; Okamura 2002) were analysed.

Statistical analysis

Statistical analysis of western blotting data for α-synuclein was performed using StatView version 5.0 for Windows (SAS Institute Inc., Cary, NC, USA). Grubb's test was used to verify the absence of outliers. The Shapiro–Wilk test and Kolmogorov–Smirnov Lilliefors test were used to verify the normality of the distribution of each variable. Two-factor analysis of variance (ANOVA) was employed to evaluate the effect of different groups (young vs. old) on α-synuclein band intensity in western blots. Differences in each band of α-synuclein protein intensity were analysed using non-paired *t*-tests. Differences in α-synuclein mRNA expression measured by quantitative RT-PCR were analysed using non-paired *t*-tests. *T*-tests were utilized to compare the number and percentage of cell bodies or fibres of GnRH single-labelled neurons and the percentage of double/triple-labelled cell bodies or fibres of neurons among all of the GnRH-positive cell bodies or fibres of neurons in the POA, ARC, or ME samples between young and old groups. The level of significance was set at $P < 0.05$. Data are expressed as means ± standard errors of the mean.

Results

Detection of α-synuclein mRNA in bovine brains and GT1-7 cells

Agarose gel electrophoresis yielded PCR products with the expected sizes, indicating the presence of *α-synuclein* in the bovine cortex, hippocampus, AH, and PH (303 bp; Fig.

1A), as well as in GT1-7 cells (306 bp; Fig. 1B). Homology search for the obtained sequences of amplified products in the gene databases revealed that the best match alignment was bovine *SNCA* (NM_001034041.2) or mouse *SNCA* (NM_001042451.2). Both had a query coverage of 100%, e-value of 0.0, and maximum alignment identity of 99%. No other bovine or mouse gene showed homology with the obtained sequences of the amplified products, confirming that the sequences of the amplified products were identical to those of bovine or mouse *SNCA*.

Quantitative RT-PCR revealed significant differences in *SNCA* mRNA expression levels between young and old bovines in the cortex and hippocampus, but not in the AH and PH (Fig. 2). These data were published recently (Niyonzima *et al.* 2024).

Detection of α-synuclein protein in the bovine brains

Western blotting confirmed the presence of α-synuclein in the young and old cortex, hippocampus, AH, and PH tissues, with differences in intensity among the sample types (Fig. 3A). The expected size of the α-synuclein monomer form was 16.6 kDa. We observed four other band sizes, most likely dimers (36.9 kDa) or oligomers (53.8 kDa, 65.2 kDa, and 91.0 kDa or 95.1 kDa). The two-factor ANOVA for all band intensities after normalisation to total protein intensity (Fig. 3B) revealed the significant effects of age on the cortex, AH, and PH, but not on the hippocampus (Fig. 3C–F). Non-paired t-tests revealed significant differences in the 36.9-kDa band for AH and PH, 65.2-kDa band for the hippocampus, and 95.1-kDa band for PH between young and old bovines. These data were published recently (Niyonzima *et al.* 2024).

Congo red staining

Congo red staining, coupled with bright-field microscopy, displayed red or orange hues in the POA and ARC of the old group, but not in the young group (Fig. 4). Some of the stained cell bodies formed clusters in the POA. Polarised light microscopy revealed red- or brown-coloured cell bodies and fibres in the old POA and ARC.

Fluorescence analysis of α-synuclein and Congo red in the cortex and hippocampus

Fluorescence immunohistochemistry detected α-synuclein in the cell bodies and fibres of neurons in the cortex and hippocampus of both the young and old groups (Fig. 5). Strong fluorescence of Congo red was detected in the cortex and hippocampus of the old group, while only weak fluorescence was detected in the young group.

Fluorescence analysis of GnRH, α-synuclein, and Congo red

Immunofluorescence immunohistochemistry followed by Congo red staining detected α-synuclein in most of the GnRH neuron cell bodies and fibres in the POA and ARC of the old group (Fig. 6B, D, F), but not the young group (Fig. 6A, C, E). Triple-positive (GnRH-positive, α-synuclein-positive, and Congo red-positive) cell bodies and fibres were abundant in the old POA (Fig. 6B), but not in the young POA (Fig. 6A); however, weak α-synuclein was occasionally observed in the young ARC and ME (Fig. 6C, 6E). The α-synuclein-positive cell bodies of GnRH neurons were observed in close proximity (within 5 μm) to cell bodies of other GnRH neurons (Fig. 6B). Only weak fluorescence of Congo red was detected in the young POA, ARC, and ME (Fig. 6A, 6C, 6E). Importantly, α-synuclein-positive GnRH fibres were observed very close to a blood vessel (Fig. 6F).

Table 2 shows the number of examined GnRH-positive, α-synuclein-positive, and Congo red-positive cell bodies and fibres in the POA, ARC, and ME regions. No significant differences were found in the number of examined GnRH-positive cell bodies and fibres between the POA and ARC. However, the number of examined GnRH-positive fibres in the ME region of older individuals was lower than that in younger individuals.

As illustrated in Table 3, the vast majority of cell bodies and fibres of GnRH neurons were positive for both α-synuclein and Congo red in the POA, ARC, and ME regions of the old group, unlike in the young group. Significant differences in almost all ratios in POA, ARC, and ME between the two groups were evident.

Discussion

The present study detected α-synuclein mRNA and protein expression in bovine AH and PH. RT-PCR also revealed the expression of α-synuclein mRNA in GT1-7 cells, and immunohistochemistry showed α-synuclein expression in bovine GnRH neurons. In the hypothalamus tissues of the old group, most of the cell bodies or fibres of GnRH neurons were α-synuclein- and Congo red-positive. To the best of our knowledge, this study is the first to report α-synuclein and Congo red positivity in the GnRH neurons of any species. The discovered α-synuclein and Congo red positivity in the POA, ARC, and ME warrants further exploration because their localization has significant implications for reproduction.

A previous study observed Congo red-positive neurons in the ARC of an old patient with Alzheimer disease (Simpson *et al*. 1988), but the corresponding cells were not identified. We observed strong α-synuclein and Congo-red signals in old GnRH neurons, but positivity for both was weak in young GnRH neurons. It is well-known that α-synuclein monomers can combine into oligomer and fibril forms, and the latter are a

484 driving cause of brain disease (Fields *et al*. 2019; Ahmed *et al*. 2022; Deyell *et al.* 2023).
485 The monomeric α-synuclein is expressed in foetal and young healthy brains (Raghavan
486 *et al.* 2004; Sulzer and Edwards 2019; Jin *et al.* 2024). Western blots in this study revealed
487 five bands, similar to a previous study on the human brain (Tong *et al*. 2010). The smallest
488 band of 16.6 kDa seemed to be correspond to the monomer because the molecular weight
489 of bovine α-synuclein is 14.5 kDa (calculated only according to the amino acid sequence
490 [NP_001029213.1], without including acetylation and phosphorylation sites stated in its
491 annotation). We speculated that the second-smallest band, 36.9 kDa, was a dimer, and the
492 band intensities of old AH and PH were significantly higher than those of young ones.
493 The band intensity of larger bands might reflect the amounts of endogenous oligomer and
494 fibril forms. The significant effect of different ages detected by two-factor ANOVA in the
495 cortex, AH, and PH suggests that further studies are required to clarify the pathogenic
496 roles of α-synuclein in GnRH neurons.

497 The toxic effects of α-synuclein within neurons include mitochondrial damage and
498 suppression of ATP synthesis (Tripathi and Chattopadhyay 2019; Wang *et al.* 2022;
499 Kinnart *et al.* 2024). Additionally, α-synuclein aggregates in lipid rafts, which are crucial
500 components of the plasma membrane, inhibiting cytoplasmic signalling pathways
501 (Perissinotto *et al.* 2020). Therefore, further studies are necessary to elucidate the
502 pathogenic mechanisms of α-synuclein, including its subcellular localisation and
503 association with cellular organelles in GnRH neurons, to clarify whether old GnRH
504 neurons exhibit damaged mitochondria, reduced ATP, and inhibited crucial receptors,
505 such as kisspeptin receptors. Importantly, α-synuclein impedes axonal transport,
506 suppressing dopamine secretion by affecting microtubules and motor proteins, leading to
507 Parkinson's disease (Lamberts *et al.* 2015). This impairment in axonal transport of GnRH

may contribute to the lower number of observable GnRH-positive fibres in older ME sections compared to younger sections. Given that whole bovine hypothalami are too large for microscopic observation, it is plausible that the total number of GnRH-positive fibres in the ME decreases with age, as previously reported in rodents (Yin *et al.* 2009). Therefore, further studies are necessary to elucidate the pathogenic mechanisms of α-synuclein using immunoelectron microscopy. The introduction of correlative light and electron microscopy is crucial for studying long GnRH neurons in large brain samples, which also contain non-GnRH neurons and glial cells (Shahmoradian *et al*. 2019; Choi *et al.*2022).

As shown in Fig. 6A and 6B, GnRH neuronal cell bodies form clusters. Most GnRH neurons (86%) form multiple close appositions with dendrites of other GnRH neurons, probably for GnRH neuronal synchronisation via dendro-dendritic communication (Campbell *et al*. 2009). Therefore, α-synuclein and Congo red positivity in GnRH neurons may indeed be relevant to the regulation of GnRH secretion by direct actions on GnRH neurons. It is known that α-synuclein suppresses cell functions in GT1-7 cells (Hsu *et al*. 2000, Zhou *et al*. 2021). Moreover, α-synuclein enters neurons by endocytosis, travels via both anterograde and retrograde axonal transport, and finally, α-synuclein is eventually secreted by exocytosis from the affected neurons (Bieri et al. 2018). Similar to prions, α-synuclein may play a critical role among clusters of GnRH neurons (Melki 2018). Therefore, further studies are warranted to clarify the roles of α-synuclein within these neurons.

GnRH neurons in the POA project to the ME and secrete GnRH into the pituitary portal blood vessels (Putteeraj *et al*. 2016). The present study found α-synuclein signals in the fibres of GnRH neurons very close to blood vessels in ME. It is known that α-

synuclein is transported into and out of the brain, even via the blood–brain barrier (Sui *et al*. 2014). Amyloid deposits were reported in the hypophyses of 7-year-old cows (Yamada *et al*. 2006). Cultured neurons can secrete α-synuclein fibrils (Gegg *et al*. 2020). Importantly, a recent study revealed that α-synuclein is misfolded in equine pituitary pars intermedia dysfunction, a common endocrine disease of aged horses (Fortin *et al*. 2021). Therefore, the findings of this study suggest another route by which α-synuclein may be secreted into the pituitary portal blood to suppress the anterior pituitary gland. Further studies are required to evaluate this hypothesis.

Similar to old human brains, old cattle brains promote brain amyloidosis and display Alzheimer's disease-like pathology (Moreno-Gonzalez *et al*. 2022). α-synuclein contributes to the formation of amyloid deposits (Yanamandra *et al*. 2011; Marsh and Blurton-Jones 2012). Recent studies have reported that confocal microscopy detects the fluorescence of Congo red, and this detection has a higher sensitivity than that of traditional bright-field or polarised light microscopy (Schultz *et al*. 2011; Scivetti *et al.* 2016; Castellani *et al.* 2017). Cytoplasmic amyloid deposits may have physiological functions (Fowler *et al*. 2006; Sergeeva and Galkin 2020). Dean and Lee (2021) reported that α-synuclein interacts with and modulates the aggregation of Pmel17, a functional amyloid in melanoma. Dharmadana *et al.* (2019) claimed that the GnRH peptide self-assembles into reversible β-sheet-based nano-fibrils, a possible functional amyloid. Therefore, the functional amyloid concept warrants further studies on GnRH neurons in the hypothalamus.

We observed the significant effect of age on α-synuclein protein expression in the AH and PH specimens, although the effect was not significant on α-synuclein mRNA expression in these specimens. Differences in post-translational modifications, including

556 ubiquitination, SUMOylation, and axonal transport of the α-synuclein protein, might
557 explain this discrepancy (Canever *et al.* 2023, Zhang *et al*. 2023). However, this study
558 faced a limitation because both the AH and PH specimens also included other brain areas
559 and nuclei, making it impossible to obtain precisely cut samples under our experimental
560 conditions. The AH tissue included SCN and SON, and the PH tissues included PVN and
561 SON; furthermore, bovine oxytocin neurons also express α-synuclein (Niyonzima *et al*.
562 2024). Therefore, the data from the western blots and RT-PCR could not exclusively
563 define α-synuclein expression in GnRH neurons. Nonetheless, RT-PCR detected α-
564 synuclein expression in the GnRH neuronal cell model GT1-7, allowing us to confidently
565 propose that bovine GnRH neurons express α-synuclein.

566 In conclusion, α-synuclein is expressed in the GnRH neurons, and there are
567 important expression differences between young and old hypothalami. Further studies on
568 how α-synuclein and amyloid act within the hypothalamus to influence GnRH secretion
569 are warranted.

570

571 **Data availability**

572 The data that support this study will be shared upon reasonable request to the
573 corresponding authors.

574

575 **Conflicts of interest**

576 The authors declare no conflicts of interest.

577

578 **Declaration of funding**

579 This research was partly supported by a Grant-in-Aid for Scientific Research [JSPS
580 Kakenhi grant number 21H02345] from the Japan Society for the Promotion of Science
581 (Tokyo, Japan) to Hiroya Kadokawa. The funder had no role in the study design, data

collection and analysis, decision to publish, and preparation of the manuscript.

Acknowledgments

We thank Yamaguchi Prefecture (Japan) for supplying the cattle brain samples. Yvan Bienvenu Niyonzima was supported by a scholarship from the Japan International Cooperation Agency (Tokyo, Japan).

References

Agriculture, forestry and fisheries Research Council secretariat (2022) Nutrition requirement. In: 'Japanese feeding standard for beef cattle'. (Eds Ministry of Agriculture, Forestry and Fisheries) pp. 51-72. (Central Association of Livestock, Industry, Tokyo, Japan) (in Japanese)

Ahmed J, Fitch TC, Donnelly CM, Joseph JA, Ball TD, Bassil MM, Son A, Zhang C, Ledreux A, Horowitz S, Qin Y, Paredes D, Kumar S (2022) Foldamers reveal and validate therapeutic targets associated with toxic α-synuclein self-assembly. *Nature Communications* **13**, 2273. doi:10.1038/s41467-022-29724-4.

Araki K, Yagi N, Aoyama K, Choong CJ, Hayakawa H, Fujimura H, Nagai Y, Goto Y, Mochizuki H (2019) Parkinson's disease is a type of amyloidosis featuring accumulation of amyloid fibrils of α-synuclein. *Proceedings of the National Academy of Sciences of the United States of America* **116**, 17963-17969. doi:10.1073/pnas.1906124116.

Bieri G, Gitler AD, Brahic M (2018) Internalization, axonal transport and release of fibrillar forms of alpha-synuclein. *Neurobiology of Disease* **109(Pt B)**, 219-225. doi: 10.1016/j.nbd.2017.03.007.

606 Bonefeld BE, Elfving B, Wegener G (2008) Reference genes for normalization: a study
607 of rat brain tissue. *Synapse (New York, N.Y.)* **62**, 302-309. doi:10.1002/syn.20496.

608 Campbell RE, Gaidamaka G, Han SK, Herbison AE (2009) Dendro-dendritic bundling
609 and shared synapses between gonadotropin-releasing hormone neurons. *Proceedings*
610 *of the National Academy of Sciences of the United States of America* **106**, 10835-
611 10840. doi:10.1073/pnas.0903463106.

612 Canever JB, Soares ES, de Avelar NCP, Cimarosti HI (2023) Targeting α-synuclein
613 post-translational modifications in Parkinson's disease. *Behavioural Brain Research*
614 **439**, 114204. doi: 10.1016/j.bbr.2022.114204.

615 Castellani C, Fedrigo M, Frigo AC, Barbera MD, Thiene G, Valente M, Adami F,
616 Angelini A (2017) Application of confocal laser scanning microscopy for the
617 diagnosis of amyloidosis. *Virchows Archiv* **470**, 455-463. doi: 10.1007/s00428-017-
618 2081-2087.

619 Choi ML, Chappard A, Singh BP, Maclachlan C, Rodrigues M, Fedotova EI,
620 Berezhnov AV, De S, Peddie CJ, Athauda D, Virdi GS, Zhang W, Evans JR, Wernick
621 AI, Zanjani ZS, Angelova PR, Esteras N, Vinokurov AY, Morris K, Jeacock K,
622 Tosatto L, Little D, Gissen P, Clarke DJ, Kunath T, Collinson L, Klenerman D,
623 Abramov AY, Horrocks MH, Gandhi S (2022) Pathological structural conversion of
624 α-synuclein at the mitochondria induces neuronal toxicity. *Nature Neuroscience* **25**,
625 1134-1148. doi: 10.1038/s41593-022-01140-3.

626 Dean DN, Lee JC (2021) Linking Parkinson's disease and melanoma: Interplay between
627 α-Synuclein and Pmel17 amyloid formation. *Movement Disorders* **36**, 1489-1498.
628 doi:10.1002/mds.28655.

629 Deyell JS, Sriparna M, Ying M, Mao X (2023) The Interplay between α-Synuclein and
630 Microglia in α-Synucleinopathies. *International Journal of Molecular Sciences* **24**,
631 2477. doi:10.3390/ijms24032477.

632 Dharmadana D, Reynolds NP, Conn CE, Valéry C (2019) pH-dependent self-assembly
633 of human neuropeptide hormone GnRH into functional amyloid nanofibrils and
634 hexagonal phases. *ACS Applied Bio Materials* **2**, 3601-3606.
635 doi:10.1021/acsabm.9b00468.

636 Epelbaum J, Terrien J (2020) Mini-review: aging of the neuroendocrine system: insights
637 from nonhuman primate models. *Progress in Neuro-psychopharmacology &*
638 *Biological Psychiatry* **100**, 109854. doi:10.1016/j.pnpbp.2024.110952.

639 Fields CR, Bengoa-Vergniory N, Wade-Martins R (2019) Targeting alpha-synuclein as
640 a therapy for Parkinson's disease. *Frontiers in Aging Neuroscience* **12**, 299.
641 doi:10.3389/fnmol.2019.00299.

642 Fortin JS, Hetak AA, Duggan KE, Burglass CM, Penticoff HB, Schott HC 2nd (2021)
643 Equine pituitary pars intermedia dysfunction: a spontaneous model of
644 synucleinopathy. *Scientific Reports* **11**, 16036. doi: 10.1038/s41598-021-95396-7.

645 Fowler DM, Koulov AV, Alory-Jost C, Marks MS, Balch WE, Kelly JW (2006)
646 Functional amyloid formation within mammalian tissue. *PLoS Biology* **4**, e6. doi:
647 10.1371/journal.pbio.0040006.

648 Gegg ME, Verona G, Schapira AHV (2020) Glucocerebrosidase deficiency promotes
649 release of α-synuclein fibrils from cultured neurons. *Human Molecular Genetics* **29,**
650 1716-1728. doi:10.1093/hmg/ddaa085.

651 Gossner AG, Foster JD, Fazakerley JK, Hunter N, Hopkins J (2011) Gene expression
652 analysis in distinct regions of the central nervous system during the development of
653 SSBP/1 sheep scrapie. *Veterinary Microbiology* **147**, 42-48.
654 doi:10.1016/j.vetmic.2010.05.043.

655 Gunes S, Hekim GN, Arslan MA, Asci R (2016) Effects of aging on the male
656 reproductive system. *Journal of Assisted Reproduction and Genetics* **33**, 441-454.
657 doi:10.1007/s10815-016-0663-y.

658 Hsu LJ, Sagara Y, Arroyo A, Rockenstein E, Sisk A, Mallory M, Wong J, Takenouchi
659 T, Hashimoto M, Masliah E (2000) Alpha-synuclein promotes mitochondrial deficit
660 and oxidative stress. *The American Journal of Pathology* **157**, 401-410.
661 doi:10.1016/s0002-9440(10)64553-1.

662 Inoue K, Hosono M, Oyama H, Hirooka H 2020. Genetic associations between
663 reproductive traits for first calving and growth curve characteristics of Japanese Black
664 cattle. *Animal Science Journal* **91**, e13467. doi:10.1111/asj.13467.

665 Jin M, Wang S, Gao X, Zou Z, Hirotsune S, Sun L (2024) Pathological and
666 physiological functional cross-talks of α-synuclein and tau in the central nervous
667 system. *Neural Regeneration Research* **19**, 855-862. doi:10.4103/1673-5374.382231.

668 Kadokawa H, Kotaniguchi M, Kereilwe O, Kitamura S (2021) Reduced gonadotroph
669 stimulation by ethanolamine plasmalogens in old bovine brains. *Scientific Reports* **11**,
670 4757. doi:10.1038/s41598-021-84306-6

671 Kadokawa H, Pandey K, Nahar A, Nakamura U, Rudolf FO（2014）Gonadotropin-
672 releasing hormone (GnRH) receptors of cattle aggregate on the surface of

673 gonadotrophs and are increased by elevated GnRH concentrations. *Animal*
674 *Reproduction Science* **150,** 84–95. doi:10.1016/j.anireprosci.2014.09.008

675 Kamomae H (2012) Reproductive disturbance. In ‘Veterinary Theriogenology’. (Eds
676 Nakao T, Tsumagari S, Katagiri S) pp. 283-340. (Buneidou Press, Tokyo, Japan) (in
677 Japanese)

678 Kereilwe O, Kadokawa H (2020a) Anti-Müllerian hormone and its receptor are detected
679 in most gonadotropin-releasing-hormone cell bodies and fibers in heifer brains.
680 *Domestic Animal Endocrinology* **72,** 106432. doi: 10.1016/j.domaniend.2019.106432.

681 Kereilwe O, Kadokawa H (2020b) Decreased Anti-Müllerian hormone and Anti-
682 Müllerian hormone receptor type 2 in hypothalami of old Japanese Black cows. T*he*
683 *Journal of veterinary medical science* **82**, 1113-1117. doi:10.1292/jvms.20-0159.

684 Kinnart I, Manders L, Heyninck T, Imberechts D, Praschberger R, Schoovaerts N,
685 Verfaillie C, Verstreken P, Vandenberghe W (2024) Elevated α-synuclein levels
686 inhibit mitophagic flux. *Nature Partner Journals Parkinson's disease* **10**, 80. doi:
687 10.1038/s41531-024-00696-0.

688 Lamberts JT, Hildebrandt EN, Brundin P (2015) Spreading of α-synuclein in the face of
689 axonal transport deficits in Parkinson's disease: a speculative synthesis. *Neurobiology*
690 *of Disease* **77**, 276-283. doi: 10.1016/j.nbd.2014.07.002.

691 Leshin LS, Rund LA, Crim JW, Kiser TE (1988) Immunocytochemical localization of
692 luteinizing hormone-releasing hormone and proopiomelanocortin neurons within the
693 preoptic area and hypothalamus of the bovine brain. *Biology of Reproduction* **39**,
694 963-975. doi:10.1095/biolreprod39.4.963.

695 Liposits Z, Merchenthaler I, Wetsel WC, Reid JJ, Mellon PL, Weiner RI, Negro-Vilar A
696 (1991) Morphological characterization of immortalized hypothalamic neurons
697 synthesizing luteinizing hormone-releasing hormone. *Endocrinology* **129**, 1575-1583.
698 doi: 10.1210/endo-129-3-1575.

699 Malhi PS, Adams GP, Pierson RA, Singh J (2006) Bovine model of reproductive aging:
700 response to ovarian synchronization and superstimulation. *Theriogenology* **66**, 1257-
701 1266. doi:10.1016/j.theriogenology.2006.02.051.

702 Marsh SE, Blurton-Jones M (2012) Examining the mechanisms that link β-amyloid and
703 α-synuclein pathologies. *Alzheimer's Research & Therapy* **4**, 11.
704 doi:10.1186/alzrt109.

705 Melki R (2018) Alpha-synuclein and the prion hypothesis in Parkinson's disease. *Revue*
706 *Neurologique* **174**, 644-652. doi:10.1016/j.neurol.2018.08.002.

707 Miyamoto, Y., Skarzynski, D.J., Okuda, K., 2000. Is tumor necrosis factor alpha a
708 trigger for the initiation of endometrial prostaglandin F(2alpha) release at luteolysis in
709 cattle? *Biology of Reproduction* **62** 1109-1115. doi:10.1095/biolreprod62.5.1109

710 Moreno-Gonzalez I, Edwards G 3rd, Morales R, Duran-Aniotz C, Escobedo G Jr,
711 Marquez M, Pumarola M, Soto C (2022) Aged cattle brain displays Alzheimer's
712 disease-likepathology and promotes brain amyloidosis in a transgenic animal model.
713 *Frontiers in Aging Neuroscience* **13,** 815361. doi:10.3389/fnagi.2021.815361.

714 Niyonzima YB, Asato Y, Kadokawa H (2024) Alpha-synuclein expression in oxytocin
715 neurons of young and old bovine brains. *Journal of Reproduction and Development.*
716 **70**, 213-222. doi: 10.1262/jrd.2024-020.

717 Obrenovich ME, Monnier VM (2004) Glycation stimulates amyloid formation. *Science*
718 *of Aging Knowledge Environment* **2004**, pe3. doi:10.1126/sageke.2004.2.pe3.

719 Okamura H (2002) Brain atlas of cattle. In 'A foundational research for elucidation and
720 estimation'. (Eds Agriculture, Forestry and Fisheries Research Council) pp.41–72.
721 (Ministry of Agriculture, Forestry and Fisheries, Tokyo, Japan) (in Japanese)

722 Osoro K, Wright IA (1992) The effect of body condition, live weight, breed, age, calf
723 performance, and calving date on reproductive performance of spring-calving beef
724 cows. *Journal of Animal Science* **70**, 1661-1666. doi:10.2527/1992.7061661x.

725 Perissinotto F, Stani C, De Cecco E, Vaccari L, Rondelli V, Posocco P, Parisse P,
726 Scaini D, Legname G, Casalis L (2020) Iron-mediated interaction of alpha synuclein
727 with lipid raft model membranes. *Nanoscale* **12**, 7631-7640.
728 doi:10.1039/d0nr00287a.

729 Puladi B, Dinekov M, Arzberger T, Taubert M, Köhler C (2021) The relation between
730 tau pathology and granulovacuolar degeneration of neurons. *Neurobiology of Disease*
731 **147**, 105138. doi:10.1016/j.nbd.2020.105138.

732 Putteeraj M, Soga T, Ubuka T, Parhar IS (2016) A "Timed" kiss is essential for
733 reproduction: Lessons from mammalian studies. *Frontiers in Endocrinology* **7**, 121.
734 doi:10.3389/fendo.2016.00121.

735 Raghavan R, Kruijff Ld, Sterrenburg MD, Rogers BB, Hladik CL, White CL 3rd (2004)
736 Alpha-synuclein expression in the developing human brain. *Pediatric and*
737 *Developmental Pathology* 7, 506-516. doi:10.1007/s10024-003-7080-9.

738 Rech R, Giaretta PR, Corrie B, de Barros CS (2018) Gross and histopathological pitfalls
739 found in the examination of 3,338 cattle brains submitted to the BSE surveillance

program in Brazil. *Pesquisa Veterinária Brasileira* **38**, 2099-2108. doi:10.1590/1678-5150-PVB-6079

Schultz SW, Nilsson KP, Westermark GT (2011) Drosophila melanogaster as a model system for studies of islet amyloid polypeptide aggregation. *PLoS One* **6**, e20221. doi: 10.1371/journal.pone.0020221.

Scivetti M, Favia G, Fatone L, Maiorano E, Crincoli V (2016) Concomitant use of Congo red staining and confocal laser scanning microscopy to detect amyloidosis in oral biopsy: A clinicopathological study of 16 patients. *Ultrastructural Pathology* **40**, 86-91. doi:10.3109/01913123.2016.1152339.

Sergeeva AV, Galkin AP (2020) Functional amyloids of eukaryotes: criteria, classification, and biological significance. *Current Genetics* **66,** 849-866. doi:10.1007/s00294-020-01079-7.

Shahmoradian SH, Lewis AJ, Genoud C, Hench J, Moors TE, Navarro PP, Castaño-Díez D, Schweighauser G, Graff-Meyer A, Goldie KN, Sütterlin R, Huisman E, Ingrassia A, Gier Y, Rozemuller AJM, Wang J, Paepe A, Erny J, Staempfli A, Hoernschemeyer J, Großerüschkamp F, Niedieker D, El-Mashtoly SF, Quadri M, Van IJcken WFJ, Bonifati V, Gerwert K, Bohrmann B, Frank S, Britschgi M, Stahlberg H, Van de Berg WDJ, Lauer ME (2019) Lewy pathology in Parkinson's disease consists of crowded organelles and lipid membranes. *Nature Neuroscience* **22**, 1099-1109. doi: 10.1038/s41593-019-0423-2.

Simpson J, Yates CM, Watts AG, Fink G (1988) Congo red birefringent structures in the hypothalamus in senile dementia of the Alzheimer type. *Neuropathology and Applied Neurobiology* **14,** 381-393. doi: 10.1111/j.1365-2990.1988.tb01140.x.

763 Sui YT, Bullock KM, Erickson MA, Zhang J, Banks WA (2014) Alpha synuclein is
764 transported into and out of the brain by the blood-brain barrier. *Peptides* **62**, 197-202.
765 doi:10.1016/j.peptides.2014.09.018.

766 Sulzer D, Edwards RH (2019) The physiological role of α-synuclein and its relationship
767 to Parkinson's Disease. *Journal of Neurochemistry* **150,** 475-486.
768 doi:10.1111/jnc.14810.

769 Tanco VM, Whitlock K, Jones MA, Wilborn RR, Brandebourg TD, Foradori CD (2016)
770 Distribution and regulation of gonadotropin-releasing hormone, kisspeptin, RF-amide
771 related peptide-3, and dynorphin in the bovine hypothalamus. *PeerJ* **4,** 1833.
772 doi:10.7717/peerj.1833.

773 Tripathi T, Chattopadhyay K (2019) Interaction of α-Synuclein with ATP Synthase:
774 Switching Role from Physiological to Pathological. *ACS Chemical Neuroscience* **10**,
775 16-17. doi:10.1021/acschemneuro.8b00407.

776 Tong J, Wong H, Guttman M, Ang LC, Forno LS, Shimadzu M, Rajput AH, Muenter
777 MD, Kish SJ, Hornykiewicz O, Furukawa Y (2010) Brain alpha-synuclein
778 accumulation in multiple system atrophy, Parkinson's disease and progressive
779 supranuclear palsy: a comparative investigation. *Brain: a Journal of Neurology* **133,**
780 172-188. doi:10.1093/brain/awp282.

781 Urbanski HF (1991) Monoclonal antibodies to luteinizing hormone-releasing hormone:
782 Production, characterization, and immunocytochemical application. *Biology of*
783 *Reproduction* **44**, 681–686. doi: 0.1095/biolreprod44.4.681

van den Beld AW, Kaufman JM, Zillikens MC, Lamberts SWJ, Egan JM, van der Lely AJ (2018) The physiology of endocrine systems with ageing. *Lancet Diabetes & Endocrinology* **6,** 647-658. doi:10.1016/S2213-8587(18)30026-3.

Wang XL, Feng ST, Wang YT, Yuan YH, Li ZP, Chen NH, Wang ZZ, Zhang Y (2022) Mitophagy, a form of selective autophagy, plays an essential role in mitochondrial dynamics of Parkinson's disease. *Cellular and Molecular Neurobiology* **42**, 1321-1339. doi: 10.1007/s10571-021-01039-w.

Yamada M, Kotani Y, Nakamura K, Kobayashi Y, Horiuchi N, Doi T, Suzuki S, Sato N, Kanno T, Matsui T (2006) Immunohistochemical distribution of amyloid deposits in 25 cows diagnosed with systemic AA amyloidosis. *The Journal of Veterinary Medical Science* **68**, 725-729. doi:10.1292/jvms.68.725.

Yanamandra K, Gruden MA, Casaite V, Meskys R, Forsgren L, Morozova-Roche LA (2011) α-synuclein reactive antibodies as diagnostic biomarkers in blood sera of Parkinson's disease patients. *PLoS One* **6**, 18513. doi:10.1371/journal.pone.0018513.

Yin W, Mendenhall JM, Monita M, Gore AC (2009) Three-dimensional properties of GnRH neuroterminals in the median eminence of young and old rats. *Journal of Comparative Neurology* **517,** 284-295. doi: 10.1002/cne.22156.

Zhang S, Zhu R, Pan B, Xu H, Olufemi MF, Gathagan RJ, Li Y, Zhang L, Zhang J, Xiang W, Kagan EM, Cao X, Yuan C, Kim SJ, Williams CK, Magaki S, Vinters HV, Lashuel HA, Garcia BA, James Petersson E, Trojanowski JQ, Lee VM, Peng C (2023) Post-translational modifications of soluble α-synuclein regulate the amplification of pathological α-synuclein. *Nature Neuroscience* **26**, 213-225. doi: 10.1038/s41593-022-01239-7.

807 Zhou S, Shen Y, Zang S, Yin X, Li P (2021) The epigenetic role of HTR1A antagonist
808 in facilitaing GnRH expression for pubertal initiation control. *Molecular therapy.*
809 *Nucleic acids* **25**, 198-206. doi:10.1016/j.omtn.2021.05.014.

810 Zussy C, Brureau A, Delair B, Marchal S, Keller E, Ixart G, Naert G, Meunier J,
811 Chevallier N, Maurice T, Givalois L (2011) Time-course and regional analyses of the
812 physiopathological changes induced after cerebral injection of an amyloid β fragment
813 in rats. *The American Journal of Pathology* **179,** 315-334.
814 doi:10.1016/j.ajpath.2011.03.021.
815

816 **Table 1.** Details of primers for bovine or mouse genes used for RT-PCR or quantitative

817 RT-PCR

Gene		Primer sequence 5'-3'	Position		Size
Species			Nucleotide	Exon	(bp)
SNCA	F	GACGCCGGGTGAGTGTG	18–34	1	303
bovine	R	CAATGCTCCCTGCTCCTTCT	301–320	4	
SNCA	F	TGCCACTGGCTTTGTCAAGA	577–596	4	306
mouse	R	AGGTACAGGACGCCGATCAC	863–882	6	
SNCA	F	GCCGGGTGAGTGTGGTGTA	21–39	1–2	80
bovine	R	GACTCCCTCCTTGGCCTTTG	81–100	2	
YWHAZ	F	AGACGGAAGGTGCTGAGAAA	256–275	2	123
bovine	R	CGTTGGGGATCAAGAACTTT	359–378	3	
SDHA	F	CATCCACTACATGACGGAGCA	428–448	5	90
bovine	R	ATCTTGCCATCTTCAGTTCTGCTA	494–517	5	

818 RT-PCR, reverse transcription-polymerase chain reaction;

819 SDHA, Succinate dehydrogenase complex flavoprotein subunit A;

820 YWHAZ, Tyrosine 3-monooxygenase/tryptophan 5-monooxygenase activation protein

821 zeta.

822

Table 2. Mean ± SEM of the number of examined GnRH-positive, α-synuclein-positive, and Congo red-positive cell bodies and fibres in the preoptic area (POA), arcuate nucleus (ARC), and median eminence (ME) of young and old groups

		Young		Old		P-value
		Mean	SEM	Mean	SEM	
Cell body in the POA	GnRH+	23.0	0.5	22.6	0.7	N.S.
	α-synuclein+	30.8	0.7	43.4	1.7	P<0.01
	Congo red+	2.2	0.2	44.0	1.8	P<0.01
Fibres in the POA	GnRH+	20.4	0.7	21.2	0.6	N.S.
	α-synuclein+	28.6	0.8	34.8	0.7	P<0.01
	Congo red+	1.6	0.2	34.4	0.7	P<0.01
Fibres in the ARC	GnRH+	20.4	0.7	18.2	1.1	N.S.
	α-synuclein+	32.0	0.9	33.8	2.3	N.S.
	Congo red+	4.2	0.6	33.6	2.3	P<0.01
Fibres in the ME	GnRH+	45.4	0.9	42.8	0.7	P<0.01
	α-synuclein+	30.2	0.6	61.8	1.0	P<0.01
	Congo red+	2.8	0.4	61.2	0.7	P<0.01

SEM: standard error of mean

N.S.: non-significant

Table 3. Mean ± SEM of the percentage of the GnRH cell body and fibres that co-localize α-synuclein or Congo red, and the percentage of α-synuclein or Congo red cells that co-localize GnRH in the young and old POA (A, B), ARC (C), and ME (D).

(A) Cell body in the POA

	Young		Old		P-value
	Mean	SEM	Mean	SEM	
GnRH cells co-localize α-synuclein	52.3	2.9	99.2	0.8	<0.01
GnRH cells co-localize Congo red	4.6	1.2	98.2	1.1	<0.01
GnRH cells co-localize both α-synuclein and Congo red	1.2	0.2	98.2	1.1	<0.01
α-synuclein cells co-localize GnRH	39.0	1.7	52.0	2.8	<0.01
Congo red cells co-localize GnRH	53.3	3.3	50.9	3.1	NS

(B) Fibres in the POA

	Young		Old		P-value
	Mean	SEM	Mean	SEM	
GnRH cells co-localize α-synuclein	56.0	2.3	95.4	2.1	<0.01
GnRH cells co-localize Congo red	3.0	1.2	92.6	3.1	<0.01
GnRH cells co-localize both α-synuclein and Congo red	0.6	0.2	92.6	3.1	<0.01
α-synuclein cells co-localize GnRH	39.8	1.1	58.1	1.0	<0.01
Congo red cells co-localize GnRH	38.3	5.0	57.0	1.5	NS

(C) Fibres in the ARC

	Young		Old		P-value
	Mean	SEM	Mean	SEM	
GnRH cells co-localize α-synuclein	56.0	2.2	97.8	1.4	<0.01
GnRH cells co-localize Congo red	4.8	1.4	97.8	1.4	<0.01
GnRH cells co-localize both α-synuclein and Congo red	1.0	0.3	87.8	4.0	<0.01
α-synuclein cells co-localize GnRH	35.6	0.8	52.7	1.2	<0.01
Congo red cells co-localize GnRH	27.0	8.6	53.1	1.7	<0.05

839

840 *(D) Fibres in the ME*

	Young		Old		P-value
	Mean	SEM	Mean	SEM	
GnRH cells co-localize α-synuclein	28.7	0.6	86.3	11.4	<0.01
GnRH cells co-localize Congo red	2.2	0.0	98.1	1.2	<0.01
GnRH cells co-localize both α-synuclein and Congo red	1.0	0.0	98.1	1.2	<0.01
α-synuclein cells co-localize GnRH	43.1	0.8	67.9	0.6	<0.01
Congo red cells co-localize GnRH	38.3	5.0	68.6	0.8	<0.01

841

842 SEM: standard error of mean

843 N.S.: non-significant

844

845 **Figure Legends**

846

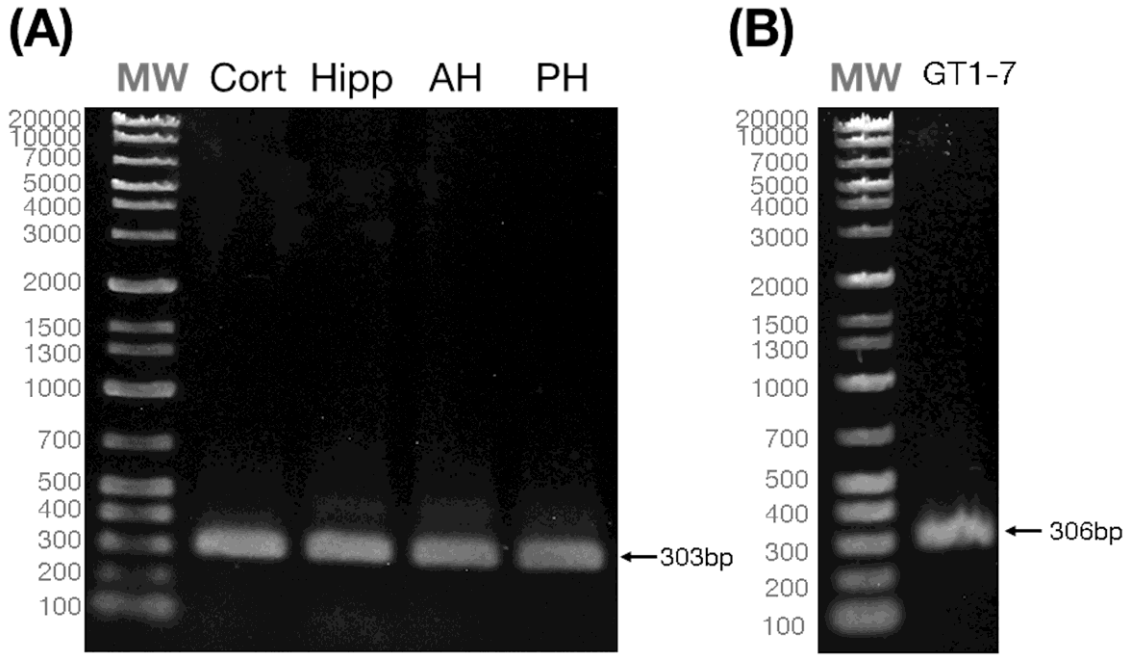

847

848 **Fig. 1.** Detection of α-synuclein mRNA in bovine brain regions (A) and GT1-7 cells (B)
849 by RT-PCR. Electrophoresis of PCR-amplified DNA products using primers for α-
850 synuclein and cDNA derived from the bovine cortex, hippocampus (Hipp), anterior
851 hypothalamus (AH), and posterior hypothalamus (PH) of post-pubertal heifers. The
852 arrows demonstrate that the sizes of the obtained DNA products met expectations—303
853 or 306 bp. The marker lane (MW) indicates the DNA marker.

854 RT-PCR: reverse transcription-polymerase chain reaction

855

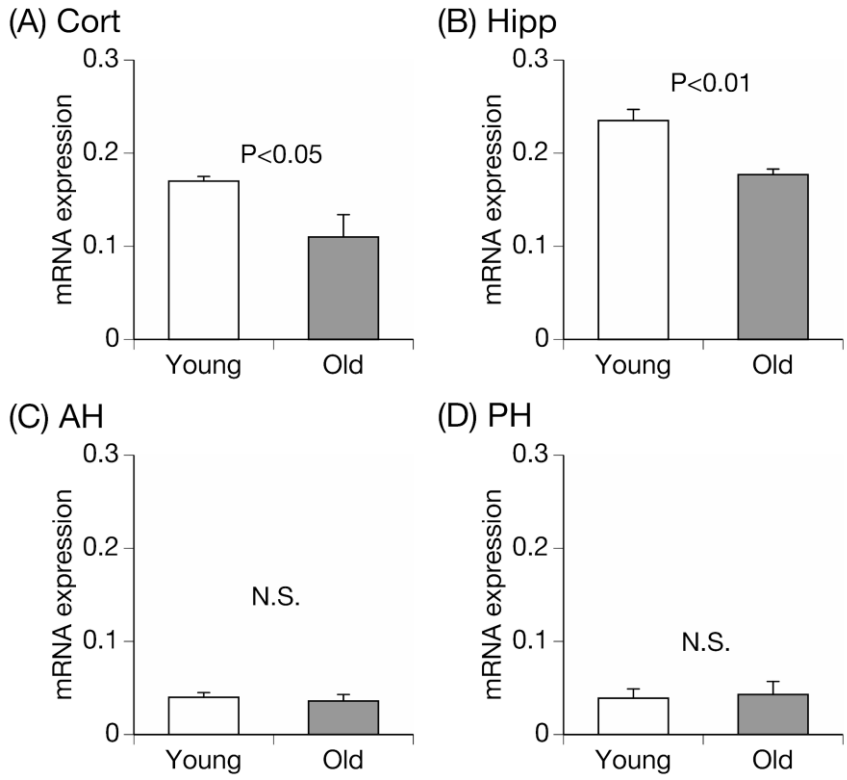

Fig. 2. Relative *SNCA* mRNA levels, presented as mean ± SEM, in various brain regions: cortex (A), hippocampus (B), anterior hypothalami (AH) (C), and posterior hypothalami (PH) (D) of healthy, post-pubertal, growing, nulliparous heifers (Young group; *n*=6) and old, multiparous cows (Old group; *n*=6), as measured by RT-qPCR. Data were normalized to the geometric means of *YWHAZ* and *SDHA* levels. The P-values in the upper end of each graph represent the results of non-paired t-tests. We obtained permission by the Journal of Reproduction and Development to re-use the graphs, which were published in another study conducted by our group (Niyonzima et al. 2024).

RT-qPCR: quantitative reverse transcription-polymerase chain reaction

SEM: standard error of mean

N.S.: non-significant

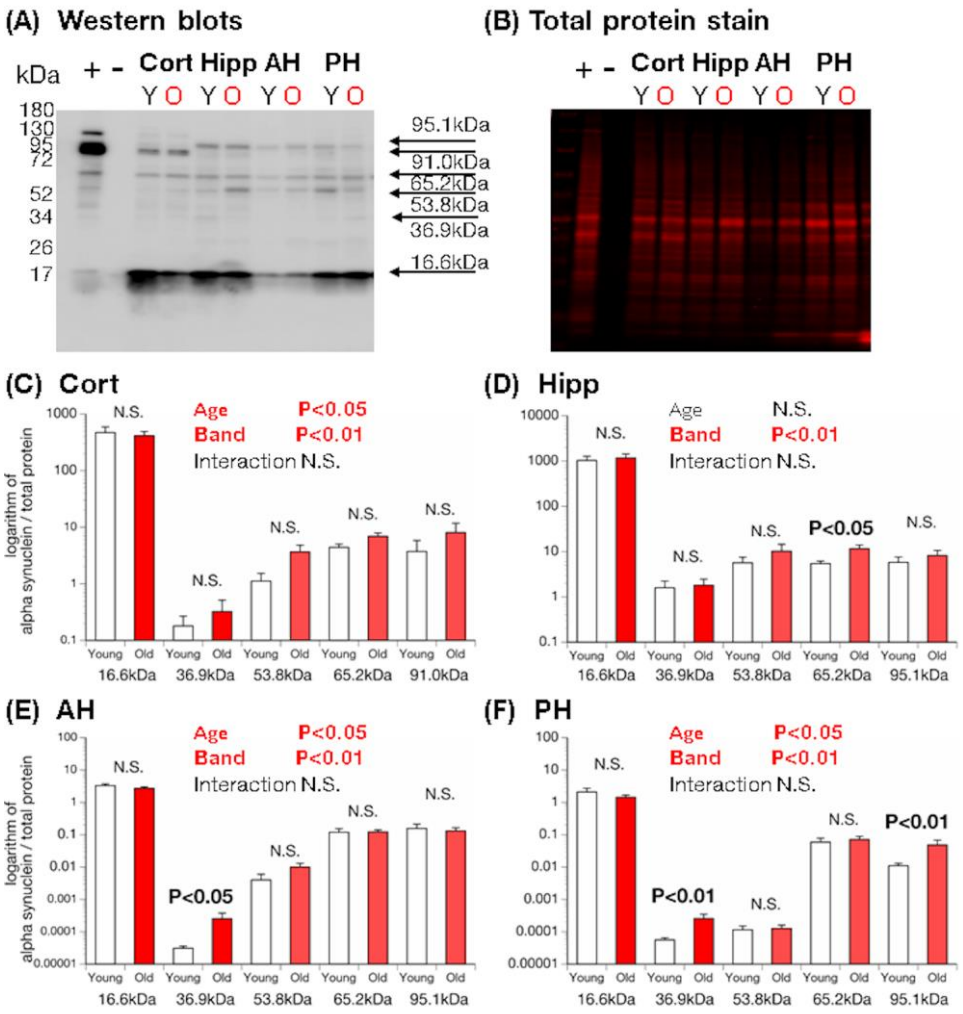

870

871 **Fig. 3.** Western blot analysis of α-synuclein in brain extracts: positive control (+, whole
872 mouse brain), negative control (-, buffer only), cortex (Cort), hippocampus (Hipp),
873 anterior hypothalami (AH), and posterior hypothalami (PH) from post-pubertal heifers
874 (Y; *n*=6) and older cows (O; *n*=6), detected with the anti-α-synuclein antibody (A).
875 Representative photos of the membrane stained by Revert 700 total protein stain (B).
876 Relative α-synuclein protein levels normalized to the amounts of total protein (C, D, E,
877 F). Headings indicate the results of two-way ANOVA. P-values indicate significant
878 differences by t-test between the young and old specimens. We obtained permission by
879 the Journal of Reproduction and Development to re-use the photos of western blots, which

were published in another study conducted by our group (Niyonzima et al. 2024).

ANOVA: analysis of variance

N.S.: non-significant

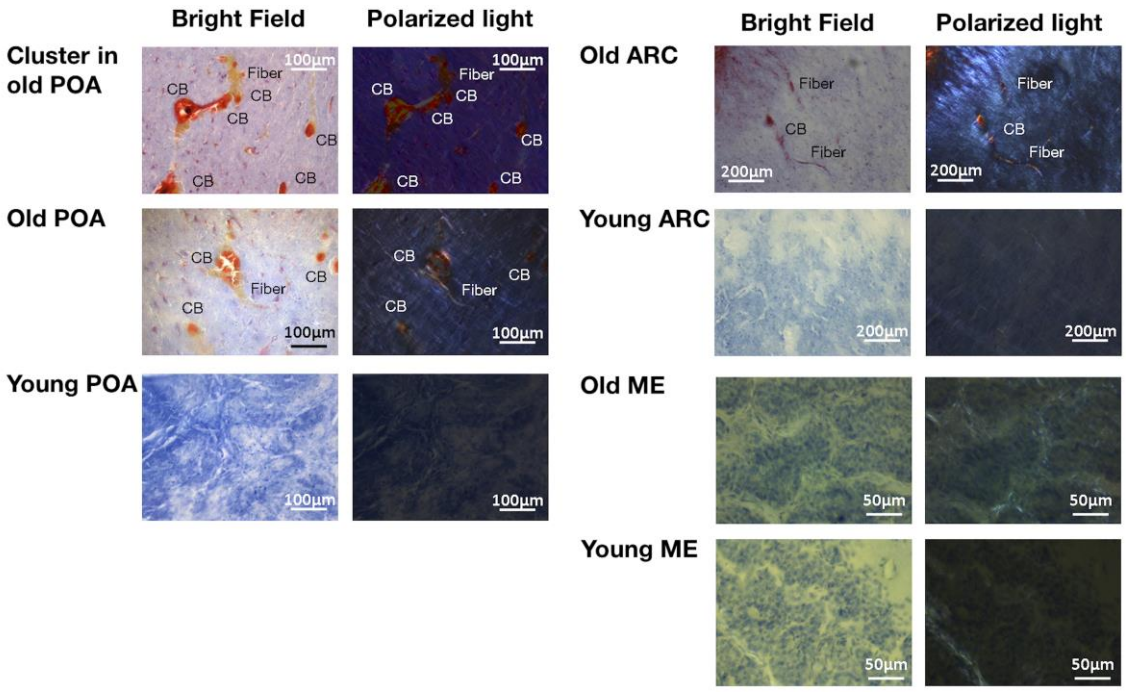

884

885

886 **Fig. 4**. Congo red staining of POA, ARC, and ME samples from young and old bovines.

887 Bright-field microscopy shows amyloid deposit regions in red. Polarized light

888 microscopy results show amyloid deposit in green or yellow. CB and Fibre indicate the

889 cell body and fibre of the neuron. Scale bars are 100 µm in POA, 200 µm in ARC, and

890 50 µm in ME.

891 POA: pre-optic area; ARC: arcuate nucleus; ME: median eminence

892

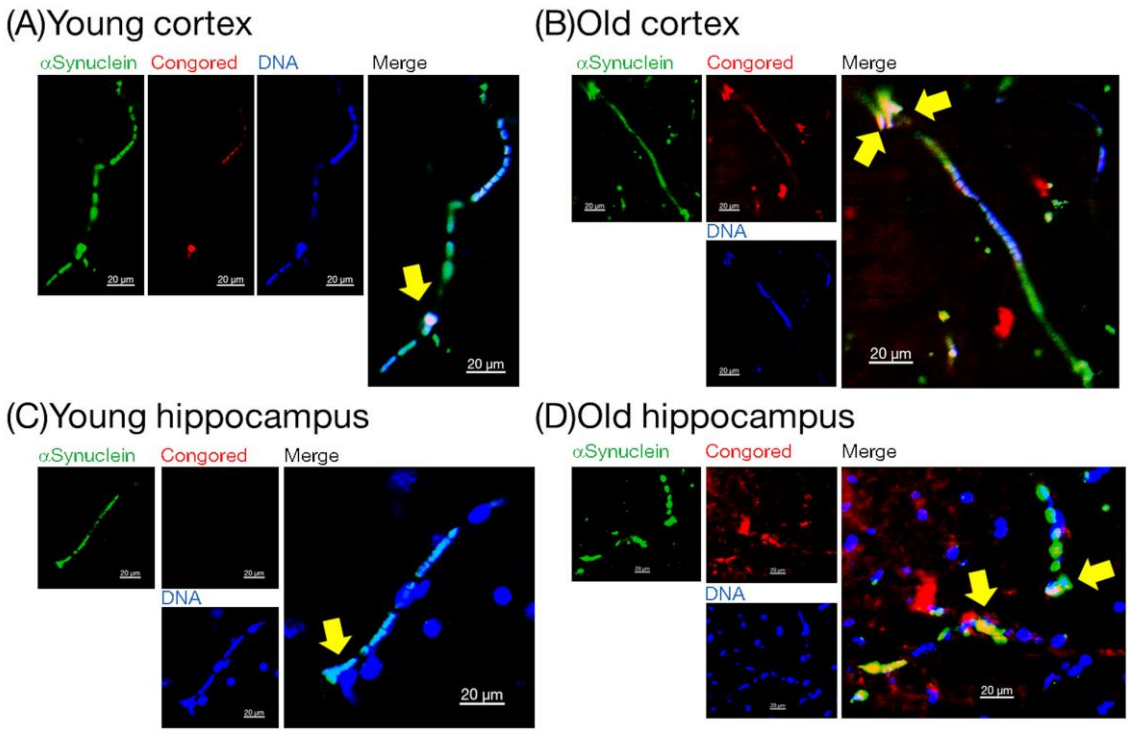

893

894

895 **Fig. 5.** Fluorescence photomicrographs of α-synuclein, Congo red, and DNA in the cortex
896 (A, B) and hippocampus (C, D) of young and old bovines. Images were captured with
897 laser confocal microscopy for α-synuclein (green), Congo red (red), and DNA (blue). In
898 the merged photos, the yellow arrows indicate the co-localisation of α-synuclein and
899 Congo red in the cell body. Scale bars, 20 μm.

900

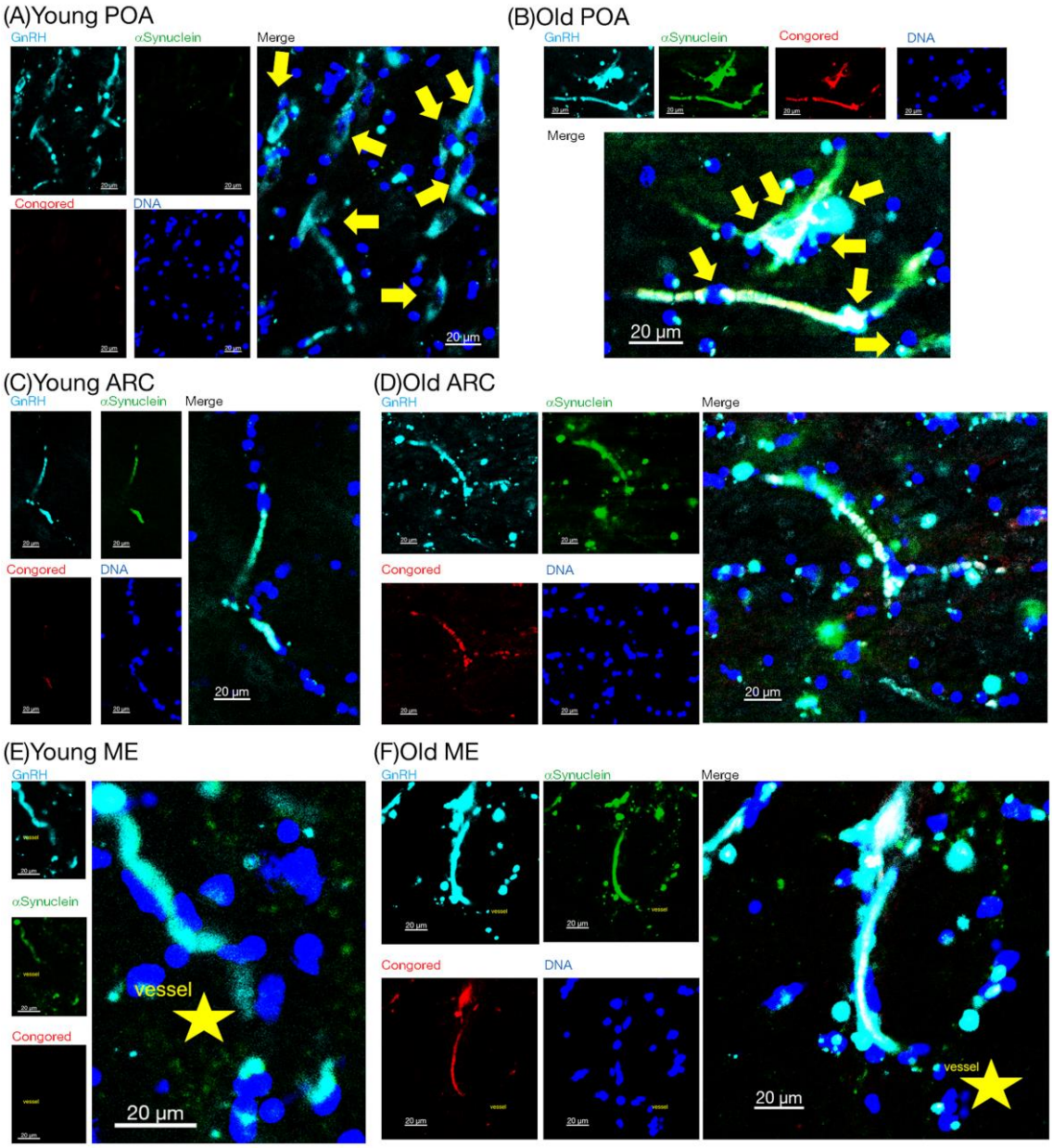

Fig. 6. Fluorescence photomicrographs of GnRH, α-synuclein, Congo red, and DNA in the POA (A, B), ARC (C, D), and ME (E, F) of young and old bovines. Images were captured with laser confocal microscopy for GnRH (light blue), α-synuclein (green), Congo red (red), and DNA (blue). In the merged photos, the yellow arrows and yellow star indicate the cell body and blood vessel. Scale bars, 20 μm.

GnRH: gonadotropin-releasing hormone; POA: pre-optic area; ARC: arcuate nucleus; ME: median eminence